# Entanglement of bosonic systems under monitored evolution

Quancheng Liu [1,2] and Klaus Ziegler [3]

[1]*State Key Laboratory of Crystal Materials, School of Physics, Shandong University, Jinan 250100, China*

[2]*Department of Physics, Institute of Nanotechnology and Advanced Materials, Bar-Ilan University, Ramat-Gan 52900, Israel*

[3]*Institut für Physik, Universität Augsburg, 86135 Augsburg, Germany*

(Received 12 May 2024; accepted 8 July 2024; published 5 August 2024)

The evolution of noninteracting bosons in the presence of repeated projective measurements is studied. Following the established approach, this monitored evolution is characterized by the first detected return and the first detected transition probabilities. We show that these quantities are directly related to the entanglement entropy and the entanglement spectrum of a bipartite system. Calculations with specific values for the number of bosons, the number of measurements, and the time steps between measurements reveal a sensitive and often strongly fluctuating entanglement entropy. In particular, we demonstrate that in the vicinity of special values for the time steps, the evolution of the entanglement entropy either is stationary or performs dynamical switching between two or more stationary values. In the entanglement spectrum, on the other hand, this complex behavior can be associated with level crossings, indicating that the dominant quantum states and their entanglement respond strongly to a change of the system parameters. We discuss briefly the role of time averaging to remove the fluctuations of the entanglement entropy.

DOI: 10.1103/PhysRevA.110.022208

## I. INTRODUCTION

Repeated measurement on a quantum system has been used to determine the first detected return (FDR) to the initial state or the first detected transition (FDT) to a state that is different from the initial state. The idea is to prepare the quantum system in an initial state $|\psi_0\rangle$, let it evolve unitarily to the state $e^{-iH\tau}|\psi_0\rangle$, and perform a projective measurement with the projector $\Pi = \mathbf{1} - |\psi\rangle\langle\psi|$, where $\mathbf{1}$ is the identity operator and $|\psi\rangle$ a state that defines the measurement. This operation yields the state $|\psi_1'\rangle = \Pi e^{-iH\tau}|\psi_0\rangle$, which either is orthogonal to $|\psi\rangle$ or vanishes when $e^{-iH\tau}|\psi_0\rangle = e^{i\varphi}|\psi\rangle$ with some phase $\varphi$. A further unitary evolution for the time $\tau$ yields $|\psi_1\rangle = e^{-iH\tau}\Pi e^{-iH\tau}|\psi_0\rangle$ and $\phi_1 = \langle\psi|\psi_1\rangle$. If $\phi_1 \neq 0$ the system was not in the state $e^{i\varphi}|\psi\rangle$ when the projection was applied. This means that our measurement to detect $|\psi\rangle$ was not successful. In this case we apply another projection to $|\psi_1\rangle$, followed by a unitary evolution to get $|\psi_2\rangle = e^{-iH\tau}\Pi|\psi_1\rangle$ and $\phi_2 = \langle\psi|\psi_2\rangle$. Again, if $\phi_2 \neq 0$ the system was not detected in the state $e^{i\varphi}|\psi\rangle$. These steps can be repeated $m$ times until $\phi_k = 0$ for all $k \geqslant m$. In other words, if the measurement is unsuccessful by not detecting the state $|\psi\rangle$, the experiment continues by another measurement, followed by the evolution for time step $\tau$. This protocol was discussed in Ref. [1] and has been applied to single-particle states to detect the particle location on a graph [2–8].

For the evolution of a system with more than one particle, the entanglement of the quantum state is a fundamental property. It can be characterized, for instance, by Rényi entropy, which measures the quantum correlations between two subsystems under a spatial bipartition [9–13]. Probing the entanglement entropy (EE) has become an important and popular concept to study measurement-induced entanglement transitions, to characterize many-body evolution and many-body localization [14–29], and to classify the topology of quantum systems.

In this paper we study the Rényi entropy in a system of noninteracting bosons, which is subject to periodically repeated projective measurements. This enables us to study the FDR and FDT probabilities, as well as the EE and entanglement spectrum (ES), and to investigate the relation between both quantities.

The focus of this paper is on the physical aspects of the monitored evolution that can also be applied to quantum computing [30]. Although quantum computing is typically based on qubits (i.e., spin states), potentially bosonic systems could also be used [31]. A promising example is photonic states. In particular, we consider $N$ noninteracting bosons, distributed in two wells which are coupled by tunneling. This can be experimentally realized as a pair of photonic cavities that are coupled by an optical fiber [32–36]. The underlying Hilbert space is $N+1$ dimensional and enables us to study the scaling behavior of the entanglement with $N$.

The structure of the paper is as follows. In Sec. II we provide a general theory with the definitions of the FDR and FDT probabilities and their relations to the reduced density matrix, the EE, and the ES. More details for the calculation of the FDR and FDT probabilities are provided in Sec. II. This includes an approach that connects the monitored evolution due to repeated measurements to the unitary evolution. The reader who is not interested in the theoretical concepts but more in the results of the monitored evolution can skip this section. In Sec. III our approach to the monitored evolution is applied to the tunneling of $N$ noninteracting bosons in a double well. For this specific model, the eigenvalues and spectral weights are calculated. In Sec. IV specific examples in terms of the parameters of the model are presented for the EE and the ES. We summarize in Sec. V.

 

## II. GENERAL CONCEPT OF PROJECTED MEASUREMENTS

The quantum system is characterized by the density operator that in the presence of repeated projective measurements reads

$$\rho^m(\tau) = \frac{1}{\mathcal{N}} e^{-iH\tau}(\Pi e^{-iH\tau})^{m-1}|\psi_0\rangle\langle\psi_0|(e^{iH\tau}\Pi)^{m-1}e^{iH\tau}, \tag{1}$$

with the normalization $\mathcal{N} = \mathrm{Tr}[e^{-iH\tau}(\Pi e^{-iH\tau})^{m-1}|\psi_0\rangle\langle\psi_0|(e^{iH\tau}\Pi)^{m-1}e^{iH\tau}]$. This density operator describes a quantum walk [37], where after each time step $\tau$ a projective measurement $\Pi$ is applied. The latter prevents the visit to the Hilbert space after a time step $\tau$ that is orthogonal to the $\Pi$-projected Hilbert space. Although in general the projector $\Pi$ is independent of the initial state $|\psi_0\rangle$ and can be chosen freely, in this paper we focus on the case discussed in the Introduction, where $\Pi$ projects onto the Hilbert space which is orthogonal to a given state $|\psi\rangle$ as $\Pi = \mathbf{1} - |\psi\rangle\langle\psi|$.

For the following discussion we start from a product space $\mathcal{H}_1 \otimes \mathcal{H}_2$ with $n_1$ bosons in the left reservoir and $n_2$ bosons in the right reservoir. Then we assume that the Hamiltonian obeys particle conservation $n_1 + n_2 = N$, which implies that it acts inside the Hilbert space that is spanned by the basis $\{|n, N-n\rangle\}_{0\leqslant n\leqslant N}$. The basis states can also contain additional quantum numbers, which are not relevant for the general discussion. In Sec. III we consider the special case in which the Hilbert space represents a double well, where $n$ bosons are in the left well and $N-n$ bosons are in the right. Then the basis is constructed from Fock states as $|n, N-n\rangle \equiv |n\rangle|N-n\rangle$ without additional quantum numbers.

Returning to the general case, in the basis $\{|n, N-n\rangle\}_{0\leqslant n\leqslant N}$ the $(N+1)\times(N+1)$ density matrix reads $\rho^m_{n,n-N;n',N-n'} = \langle n, N-n|\rho^m(\tau)|n', N-n'\rangle$, with $n, n' = 0, \ldots, N$. After summing over all basis states of $\mathcal{H}_2$, the reduced density matrix $\hat\rho$ becomes an $(N+1)\times(N+1)$ diagonal matrix with elements

$$\begin{aligned}\hat\rho^m_{nn} &= \sum_{n'=0}^{N}\langle n, n'|\rho^m(\tau)|n, n'\rangle = \langle n, N-n|\rho^m(\tau)|n, N-n\rangle \\ &= \frac{1}{\mathcal{N}}\langle n, N-n|e^{-iH\tau}(\Pi e^{-iH\tau})^{m-1}|\psi_0\rangle \\ &\quad\times\langle\psi_0|(e^{iH\tau}\Pi)^{m-1}e^{iH\tau}|n, N-n\rangle.\end{aligned} \tag{2}$$

With the projector $P_n := |n, N-n\rangle\langle n, N-n|$ the density matrix elements can also be written as a trace expression

$$\hat\rho^m_{nn} = \frac{1}{\mathcal{N}}\mathrm{Tr}[P_n e^{-iH\tau}(\Pi e^{-iH\tau})^{m-1}P_0(e^{iH\tau}\Pi)^{m-1}e^{iH\tau}], \tag{3}$$

where we have assumed $|\psi_0\rangle = |0, N\rangle$ for the initial state. One should note that the right-hand side of Eq. (2) with $\Pi$ replaced by $\Pi_n = \mathbf{1} - P_n$ is either the FDR probability (for $n = 0$) or the FDT probability (for $n > 0$). Therefore, known results of the FDR and FDT probabilities [6,38,39] can be directly used for the reduced density matrix through the relation

$$\hat\rho^m_{nn} = \frac{|\phi_{m;n0}|^2}{\sum_{n=0}^{N}|\phi_{m;n0}|^2}, \tag{4}$$

with the FDT amplitude for $|0, N\rangle \to |n, N-n\rangle$ $(n \neq 0)$ after $m$ measurements

$$\phi_{m;n0} := \langle n, N-n|e^{-iH\tau}(\Pi_n e^{-iH\tau})^{m-1}|0, N\rangle \tag{5}$$

and the corresponding FDR amplitude $\phi_{m;00}$ for $|0, N\rangle \to |0, N\rangle$. It is crucial to note that $\sum_{n=0}^{N}|\phi_{m;n0}|^2 \leqslant 1$ for $m > 1$ due to the projection $\Pi$. Some known results for the FDR and FDT amplitudes are summarized in Sec. II.

With this expression for $\hat\rho^m_{nn}$ we can introduce the Rényi entropy [23] as a quantitative measure for the entanglement of the two Hilbert spaces $\mathcal{H}_1$ and $\mathcal{H}_2$,

$$\mathcal{S}_\alpha(\tau, N, m) = \frac{1}{1-\alpha}\log_2\mathrm{Tr}[(\bar\rho^m)^\alpha(\tau)]. \tag{6}$$

In general, $\alpha$ is a free parameter and typical values used are $\alpha = 2, 3$ [23]. For the subsequent calculations we set $\alpha = 2$, i.e., we calculate $\mathcal{S}_2(\tau, N, m)$ as the EE.

While the EE reveals a global measure for the monitored evolution, the ES [40] provides a local measure of the evolution for the transition between individual states $|0, N\rangle \to |n, N-n\rangle$. In other words, it reveals the contribution of individual states to the entangled state of the evolving quantum system. It is defined as the logarithm of the reduced density matrix eigenvalues. In the present case the reduced density matrix is already diagonal such that

$$\xi_{m;n} = -\ln\left(\bar\rho^m_{nn}\right) = -2\ln(|\phi_{m;n0}|) + \ln\left(\sum_{n=0}^{N}|\phi_{m;n0}|^2\right). \tag{7}$$

The smallest value of $\xi_{m;n}$ corresponds to the dominant transition $|0, N\rangle \to |n, N-n\rangle$ after $m$ measurements. A crossing of the lowest levels upon changing the time step $\tau$ or $m$ is reminiscent of a phase transition in classical statistical systems due to a crossing of the ground-state energies.

The FDR or FDT amplitude in Eq. (5) is written in the Fock basis. It is convenient to express the evolution operator in the eigenbasis $\{|E_k\rangle\}$ of the Hamiltonian as

$$\begin{aligned}\phi_{m;n0} = \sum_{\{k_j=0\}}^{N}&\langle\psi_n|E_{k_1}\rangle e^{-iE_{k_1}\tau}\langle E_{k_1}|\Pi_n|E_{k_2}\rangle e^{-iE_{k_2}\tau} \\ &\cdots\langle E_{k_{m-1}}|\Pi_n|E_{k_m}\rangle e^{-iE_{k_m}\tau}\langle E_{k_m}|\psi_0\rangle.\end{aligned} \tag{8}$$

For the projector $\Pi_n = \mathbf{1} - |n, N-n\rangle\langle n, N-n|$, a typical matrix element then reads

$$\begin{aligned}&\langle E_k|(\mathbf{1} - |n, N-n\rangle\langle n, N-n|)|E_{k'}\rangle \\ &\quad= \delta_{kk'} - q^*_{n,k}q_{n,k'} =: (\mathbf{1} - Q^*_n E Q_n)_{kk'},\end{aligned} \tag{9}$$

with $q_{n,k} = \langle n, N-n|E_k\rangle$ and $q^*_{n,k} = \langle E_k|n, N-n\rangle$. Here $E$ is the $(N+1)\times(N+1)$ matrix, whose matrix elements are 1. Moreover, $Q_n$ is a diagonal matrix, consisting of the elements $\{q_{n,k}\}$. Then the FDR or FDT amplitude of Eq. (5) can be written as

$$\phi_{m;n0} = \sum_{k,k'=0}^{N} q_{n,k}D_k[(\mathbf{1} - Q^*_n E Q_n)D]^{m-1}_{kk'}q^*_{0,k'}, \tag{10}$$

with $D_k = e^{-iE_k\tau}$. It should be noted that $(Q^*_n)^{-1}(D - Q^*_n E Q_n D)^{m-1}Q^*_n$ is a function of $Q_n Q^*_n$ (cf. Ref. [41]): Since

$Q_n$ and $D$ are diagonal matrices, they commute and we get the relation

$$(D - Q_n^* E D Q_n)^{m-1} = Q_n^* (D - E D Q_n Q_n^*)^{m-1} (Q_n^*)^{-1}, \quad (11)$$

which is proved by complete induction. Moreover, we can write $(D - Q_n^* E D Q_n)^{m-1} = D^{-1/2} T_n^{m-1} D^{1/2}$, with $T_n := D^{1/2}(\mathbf{1} - Q_n^* E Q_n) D^{1/2}$, and for Eq. (10)

$$\phi_{m;n0} = \mathrm{Tr}\big(D^{1/2} T_n^{m-1} D^{1/2} Q_0^* E Q_n\big). \quad (12)$$

Thus, the matrix $T_n$ represents the monitored evolution under repeated measurements, which is the analog of the unitary evolution matrix $U = \exp(-iH\tau)$ in the Fock basis. Its largest eigenvalues control the large-$m$ (i.e., stationary) behavior of $\phi_{m;n0}$, while the smaller eigenvalues decay quickly. Therefore, the task is to identify those largest eigenvalues for the given parameters of the model.

The matrix $T_n$ has some important properties that are useful for the calculation of $\phi_{m;n0}$. First, since $\sum_k q_{n,k} q^*_{n',k} = \delta_{nn'}$, there is a complete set of right and left eigenvectors of the Hermitian matrix $\mathbf{1} - Q_n^* E Q_n$ with an eigenvalue 0 and $N$ eigenvalues 1 due to

$$\sum_{k'} (\delta_{kk'} - q^*_{n,k} q_{n,k'}) q^*_{n',k'} = (1 - \delta_{nn'}) q^*_{n',k},$$
$$\sum_{k} q_{n',k} (\delta_{kk'} - q^*_{n,k} q_{n,k'}) = (1 - \delta_{nn'}) q_{n',k'}. \quad (13)$$

Defining the vector $\mathbf{q}_n := (q_{n,0}, q_{n,1}, \ldots, q_{n,N})^T$, we get $Q_n^* E Q_n \mathbf{q}^*_{n'} = \mathbf{q}_n \delta_{nn'}$, which implies, for the vector $\mathbf{x} := \sum_{n'} a_{n'} D^{-1/2} \mathbf{q}^*_{n'}$,

$$T_n \mathbf{x} = \begin{cases} D\mathbf{x} & \text{for } a_n = 0 \\ 0 & \text{for } a_{n'} = 0 \ (n' \neq n). \end{cases} \quad (14)$$

It is possible that $T_n \mathbf{x} = D\mathbf{x}$ reduces to $T_n \mathbf{x} = e^{i\varphi}\mathbf{x}$ when we have $D\mathbf{x} = e^{i\varphi}\mathbf{x}$, which can happen in the presence of degenerate $E_j\tau \ (\mathrm{mod} 2\pi)$ or when some components of the vectors $\mathbf{q}_{n'}$ vanish. In this case $\mathbf{x}$ is an eigenvector of $T_n$ whose eigenvalue lies on the unit circle of the complex plane. This means that $\mathbf{x}$ does not decay but accumulates only a phase. This eigenvector does not contribute to the FDR or FDT amplitude though, since $\mathbf{x}$ is orthogonal to $\mathbf{q}_n$ and therefore $E Q_n \mathbf{x} = 0$.

Besides these special vectors, the eigenvalues of $T_n$ can be quite complex in general. On the other hand, even a two-level system (i.e., $N = 1$ and $n = 0, 1$) with energies $E_{0,1}$ is already instructive. In this case $T_n$ has two eigenvalues

$$\lambda_0 = 0, \quad \lambda_1 = (1 - |q_{n,0}|^2) e^{-2iE_0\tau} + |q_{n,0}|^2 e^{-2iE_1\tau}, \quad (15)$$

where $|q_{n,1}|^2 = 1 - |q_{n,0}|^2$ and $|\lambda_1|^2 = 1 - 2(1 - |q_{n,0}|^2)|q_{n,0}|^2 \{1 - \cos[2(E_1 - E_0)\tau]\}$. Thus, the eigenvalues of $T_n$ are on the unit disk, one at the center and the other one only for special values on the unit circle, namely, for $|q_{n,0}| = 0, 1$ and/or for $(E_1 - E_0)\tau = 0 \ (\mathrm{mod}\pi)$. This means that, except for the special values with $|\lambda_1| = 1$, $T_n^{m-1}$ decays exponentially fast. We will see subsequently that this type of behavior exists also for larger systems. In particular, we will study a system of $N$ noninteracting bosons.

### FDR and FDT amplitudes

Next we discuss the connection between the unitary and the monitored evolution by a linear relation. We consider only the FDR or FDT amplitude, since this is the building block for the other physical quantities, according to our discussion in the preceding section. The first detected passage time problem, as discussed in Refs. [1,4] for a single particle on a tight-binding graph, can be directly generalized to the evolution in a general Hilbert space. The unitary evolution of the transition $|\psi_0\rangle \to |\psi_n\rangle$ for the time $\tau$ provides the amplitudes

$$v_m := \phi_{1;n0}(m\tau) = \langle \psi_n | e^{-iHm\tau} | \psi_0 \rangle,$$
$$u_m := \phi_{1;00}(m\tau) = \langle \psi_0 | e^{-iHm\tau} | \psi_0 \rangle. \quad (16)$$

There exists a mapping from the unitary amplitudes in Eq. (16) to the FDR or FDT amplitudes $\phi_{m;n0}$ as (cf. Appendix B)

$$\vec{\phi} = (\mathbf{1} + \Gamma)^{-1} \vec{v}, \quad (17)$$

with the $m$-component vectors $\vec{\phi} = (\phi_{1;n0}, \phi_{2;n0}, \ldots, \phi_{m;n0})$ and $\vec{v} = (v_1, v_2, \ldots, v_m)$ and with the triangular matrix $\Gamma$ whose elements are

$$\Gamma_{ij} = \begin{cases} u_{i-j} & \text{for } 1 \leqslant i - j \leqslant m - 1 \\ 0 & \text{otherwise.} \end{cases} \quad (18)$$

In other words, the FDR or FDT amplitudes can be recursively constructed from the unitary amplitudes in Eq. (17). This is solved by a discrete Fourier transformation with

$$\sum_{m \geqslant 1} z^m \phi_{m;n0} = \hat{\phi}(z) = \frac{\hat{v}(z)}{1 + \hat{u}(z)} \quad (19)$$

for $z$ inside the complex unit disk (i.e., $|z| < 1$) and with the Fourier transformed unitary amplitudes of Eq. (16):

$$\hat{u}(z) = z \sum_{j=0}^{N} \frac{|\langle \Psi_0 | E_j \rangle|^2}{e^{iE_j\tau} - z}, \quad \hat{v}(z) = z \sum_{j=0}^{N} \frac{\langle \Psi | E_j \rangle \langle E_j | \Psi_0 \rangle}{e^{iE_j\tau} - z}. \quad (20)$$

The advantage of using a continuous function $\hat{\phi}(z)$ rather than a discrete function $\phi_{m;n0}$ is that analytic tools, such as integration or perturbation theory, can be employed to exploit its properties.

Once the function $\hat{\phi}(z)$ is known, $\phi_{m;n0}$ can be retrieved as the residue of the Cauchy integral: Since $\hat{\phi}(z)$ does not have poles inside the unit disk due to $1 + \hat{u} = \sum_j |\langle \Psi_0 | E_j \rangle|^2 / [1 - z \exp(-iE_j\tau)]$, the FDR or FDT amplitude reads

$$\phi_{m;n0} = \frac{1}{2\pi i} \int_C z^{-m-1} \frac{\hat{v}}{1 + \hat{u}} dz, \quad (21)$$

with a contour $C$ around $z = 0$ smaller than the unit circle in order to avoid the poles of $\hat{v}/(1 + \hat{u})$. The function $\hat{\phi}_u = \hat{u}/(1 + \hat{u})$ is a unimodular function of the form $\hat{\phi}_u(e^{i\omega}) = e^{if(\omega)}$ with a characteristic winding number that is equal to the dimensionality of the underlying Hilbert space in the absence of degeneracies for $E_j\tau \ (\mathrm{mod} 2\pi)$ [6]. The example of $N = 8$ noninteracting bosons is visualized in Fig. 1.

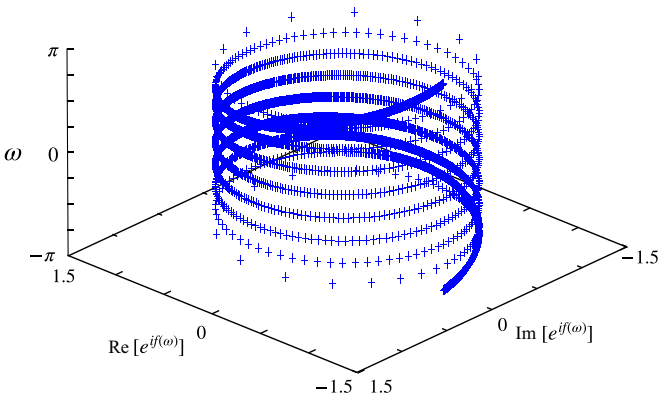


FIG. 1. Plot of $\hat{\phi}_r(e^{i\omega}) = e^{if(\omega)}$ for $-\pi \leqslant \omega < \pi$ (vertical axis) with winding number 9 for eight noninteracting bosons. The density of points is inverse to the sensitivity of the phase $f(\omega)$ to a change of $\omega$.

## III. PHYSICAL MODEL: NONINTERACTING BOSONS IN A DOUBLE WELL

Within the single-mode approximation [42], the double well with $N$ bosons can be described as a two-site Bose model

$$H = -J(a_l^\dagger a_r + a_r^\dagger a_l), \tag{22}$$

where $a_{L,R}^\dagger$ ($a_{L,R}$) are the bosonic creation (annihilation) operators in the left or right potential wells, with $n_{l,r} = a_{l,r}^\dagger a_{l,r}$ the corresponding number operators, and $J$ is the tunneling rate of bosons between the two wells. Using Fock states $|n, N-n\rangle \equiv |n\rangle|N-n\rangle$ ($n = 0, \ldots, N$) as a basis of the Hilbert space, the corresponding Hamiltonian matrix has a tridiagonal structure with

$$\begin{aligned} H_{n,n'} &= \langle n, N-n|H|n', N-n'\rangle \\ &= -J\sqrt{n(N+1-n)}\delta_{n,n'-1} - J\sqrt{n'(N+1-n')}\delta_{n,n'+1}. \end{aligned} \tag{23}$$

These matrix elements represent an $(N+1)$-site tight-binding chain with broken translational invariance and nearest-neighbor tunneling rates $-J\sqrt{n(N+1-n)}$. The sites $n$ and $n'$ are connected by hopping of a single particle.

For noninteracting bosons we can calculate $\hat{\rho}_{m;nn}$ explicitly, since the energy levels and the spectral weight factors $\langle n, N-n|E_k\rangle$ are known. This system can be realized for photons at a beam splitter [43,44] or in two harmonic cavities, which are connected through an optical fiber [32–36]. Then the tunneling Hamiltonian $H = -J(a_l^\dagger a_r + a_r^\dagger a_l)$ for $N$ bosons has $N+1$ equidistant energy levels $E_k = -J(N-2k)$ ($k = 0, 1, \ldots, N$) with eigenstates

$$|E_k\rangle = \frac{2^{-N/2}}{\sqrt{k!(N-k)!}}(a_l^\dagger + a_r^\dagger)^k(a_l^\dagger - a_r^\dagger)^{N-k}|0,0\rangle, \tag{24}$$

where the normalization follows directly from $(a^\dagger)^l|0\rangle = \sqrt{l!}\,|l\rangle$. Thus, the fastest oscillations occur with frequency $NJ$ and the characteristic parameter for the evolution is $J\tau$. The spectral weights $q_{n,k} := \langle n, N-n|E_k\rangle$ are explicitly calculated in Eq. (A2) of Appendix A. In particular, for the special cases $n = 0$ and $n = N$ we have

$$\begin{aligned} q_{0,k} &= 2^{-N/2}\frac{\sqrt{N!}}{\sqrt{k!(N-k)!}}(-1)^{N-k}, \\ q_{N,k} &= 2^{-N/2}\frac{\sqrt{N!}}{\sqrt{k!(N-k)!}}. \end{aligned} \tag{25}$$

These specific expressions can be entered into the FDR or FDT amplitude $\phi_{m;n0}$ of Eq. (12), using $D_k = e^{-iE_k\tau} = e^{iJ(N-2k)\tau}$. Moreover, $Q_n$, the diagonal matrix with elements $q_{n,k}$ for fixed $n$, is real here, which enables us to write

$$\begin{aligned} \phi_{m;n0} &= \mathrm{Tr}[D(D - Q_nEDQ_n)^{m-1}Q_0^*EQ_n] \\ &= \mathrm{Tr}[D^{1/2}T^{m-1}D^{1/2}Q_0^*EQ_n]. \end{aligned} \tag{26}$$

This gives immediately the reduced density matrix of Eq. (4), the EE of Eq. (6), and the ES of Eq. (7). Some examples for the eigenvalues of the monitored evolution matrix $T$ are presented in Fig. 2.

Returning to the unitary evolution, the amplitudes $u_m$ and $v_m$ of Eq. (16) are determined by multiples of the frequency $J\tau$,

$$\begin{aligned} u_m &= \langle 0, N|e^{-iHm\tau}|0, N\rangle = \cos^N(mJ\tau), \\ v_m &= \langle N, 0|e^{-iHm\tau}|0, N\rangle = (-i)^N \sin^N(mJ\tau), \end{aligned} \tag{27}$$

which are periodic with $m\tau J/\hbar = 2\pi$ or periodic with $m\tau J/\hbar = \pi$ for even $N$ (cf. Fig. 3). For a very short time (i.e., for $mJ\tau \ll 1/\sqrt{N}$) we have a Gaussian decay of the Fock state $|0, N\rangle$ as

$$u_m = \cos^N(mJ\tau) \sim e^{-Nm^2J^2\tau^2/2}, \tag{28}$$

as also illustrated in Fig. 3. This nonexponential behavior in $\tau$ reflects the quantum Zeno effect [45]. Finally, the Fourier transformed unitary amplitudes for $|\psi_0\rangle = |0, N\rangle$ and $|\psi\rangle = |N, 0\rangle$ read

$$\begin{aligned} \hat{u}(z) &= 2^{-N}\sum_{k=0}^{N}\binom{N}{k}\frac{z}{e^{iE_k\tau} - z}, \\ \hat{v}(z) &= (-2)^{-N}\sum_{k=0}^{N}\binom{N}{k}\frac{(-1)^k z}{e^{iE_k\tau} - z}. \end{aligned} \tag{29}$$

They can be used to calculate the FDR or FDT amplitudes as the residue of the corresponding Cauchy integrals.

## IV. DISCUSSION OF THE RESULTS

The results of the preceding section will now be used to calculate the FDR or FDT probabilities, the EE, and the ES for specific realizations of the model. To this end we note that the parameters of the bosonic system are the number of bosons $N$, the number of measurements $m-1$, and the time steps between measurements $\tau$. The latter always appears in combination with the tunneling rate $J$ as $J\tau$. This is a consequence of the fact that we have noninteracting bosons, where tunneling is the only mechanism of the evolution. The combination $J\tau/\hbar$ provides a dimensionless time step in our system, which we will use subsequently.

The characteristic features of the unitary dynamics defined in Eq. (27) are visualized in Fig. 3, which indicates a smooth

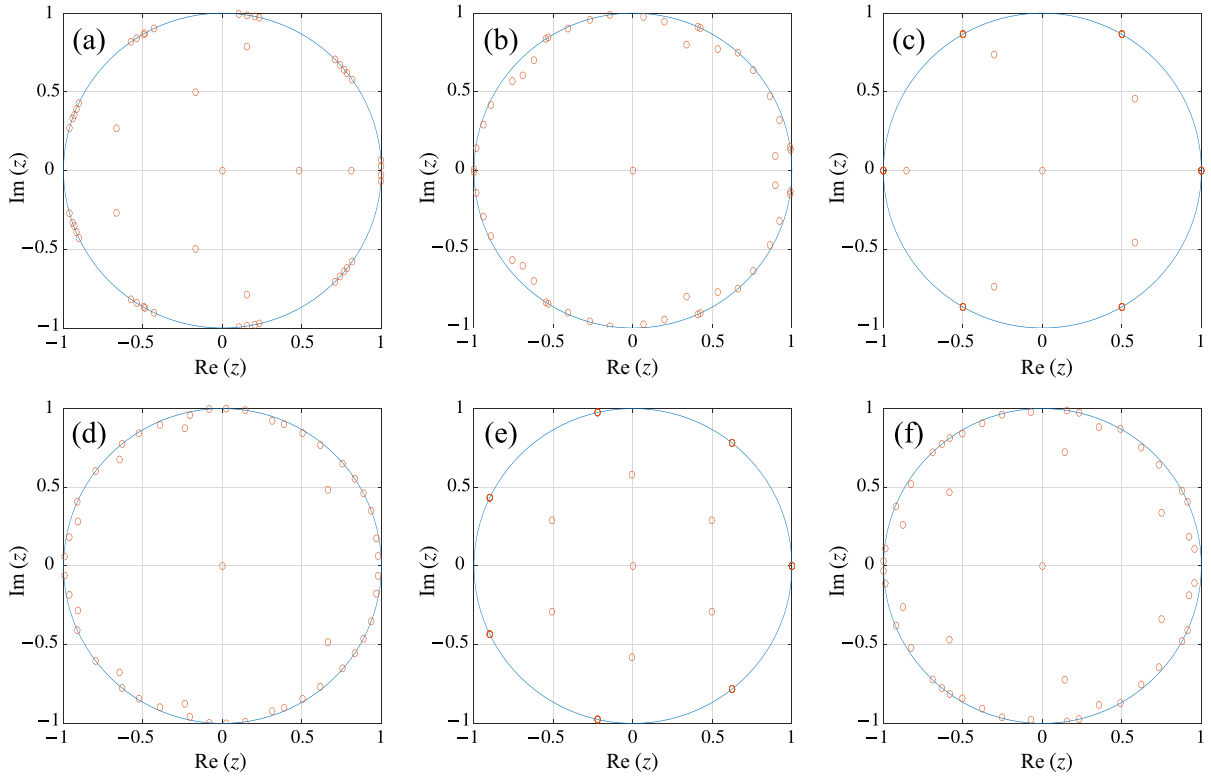


FIG. 2. Plots of 51 eigenvalues $z$ of $T$ for $N = 50$ bosons with (a) $J\tau = 0.7\hbar$, (b) $J\tau = 0.5\hbar$, (c) $J\tau = \pi\hbar/6$, (d) $J\tau = (\pi/6 + 10^{-2})\hbar$, (e) $J\tau = \pi\hbar/7$, and (f) $J\tau = (\pi/7 + 10^{-2})\hbar$. Very small changes in $J\tau$ have a strong effect on the eigenvalues and their degeneracy. This can be seen by comparing (c) and (d) or (e) and (f).

variation of the amplitudes over time for the return to the initial state $|0, N\rangle \to |0, N\rangle$ and for the transition of all bosons to the other well $|0, N\rangle \to |N, 0\rangle$. This periodic behavior is also reflected by the unitary evolution of the EE in Fig. 4(a), which vanishes when all bosons are either in the left or in the right well. Repeated measurements will substantially affect this periodic behavior.

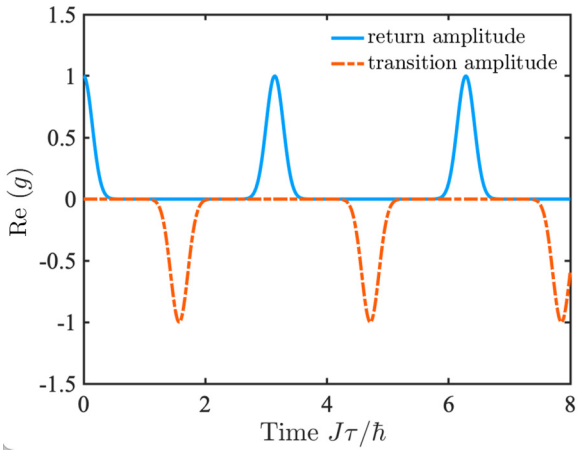


FIG. 3. Unitary evolution. Real parts of the return amplitude $u_1(\tau)$ ($|0, N\rangle \to |0, N\rangle$) and the transition amplitude $v_1(\tau)$ ($|0, N\rangle \to |N, 0\rangle$) are plotted as a function of the dimensionless time $J\tau/\hbar$ for 50 noninteracting bosons.

Without measurement (i.e., for $m = 1$) the EE is determined by the unitary amplitudes for all transitions $|0, N\rangle \to |n, N - n\rangle$, which are smooth and periodic in time

$$\phi_{1,n0} = e^{iNJ\tau} \sum_{k=0}^{N} e^{-2ikJ\tau} q_{n,k} q_{0,k}. \tag{30}$$

This expression, together with Eq. (A4), gives, for $J\tau = 0 \pmod{2\pi}$ and $J\tau/\hbar = \pi \pmod{2\pi}$,

$$\phi_{1,n0} = e^{iNJ\tau} \delta_{n0}, \tag{31}$$

implying $\mathcal{S}_2(\tau, N, 1) = 0$. This is reflected in the plot of $\mathcal{S}_2(\tau, N, 1)$ of Fig. 4(a), which indicates also a vanishing EE at $J\tau/\hbar = \pi/2 \pmod{2\pi}$. The periodicity does not depend on the number of bosons $N$, while the value of the EE increases with $N$. This is remarkable because the eigenvalues as well as the weight $q_{n,k}$ depend strongly on $N$. The behavior of the EE is affected by measurements depending on the time steps between the measurements. As visualized in Fig. 4(b) for $N = 20$ bosons, for a very short time step $J\tau/\hbar$ between measurements, the periodic behavior of the unitary evolution disappears. The corresponding ES in Fig. 5 reveal that the level crossings are more complex in the case of the monitored evolution and they take place on a much shorter timescale.

As already mentioned in the discussion of the FDR and FDT probabilities, the unitary evolution between measurements is characterized by the phase factor $\exp(-iJ\tau m/\hbar)$, which is periodic for $m = l$ if $J\tau = 2\pi\hbar/l$. In other words,

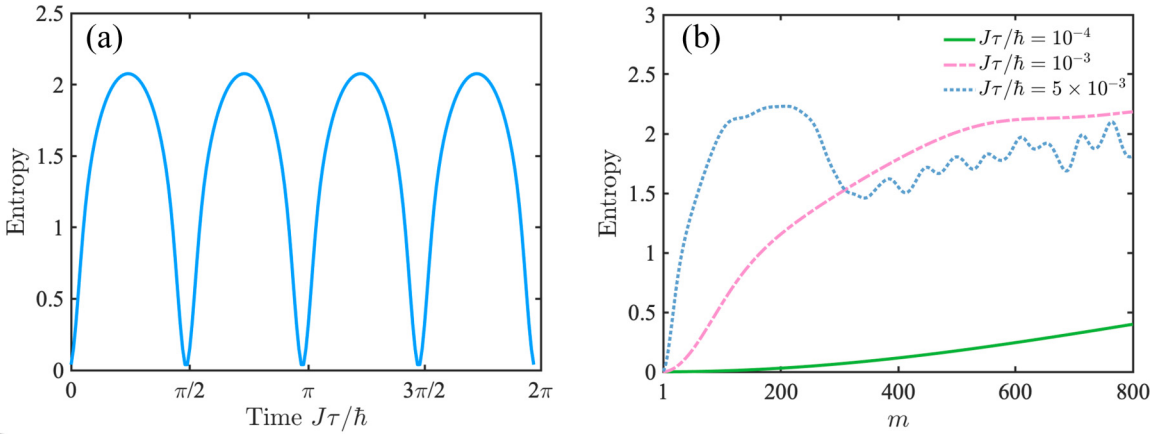


FIG. 4. (a) The unitary evolution of $N = 20$ bosons for the time $J\tau/\hbar$ is periodic. (b) The monitored evolution of the entanglement entropy for a high frequency of measurements reflects the quantum Zeno effect, where an increasing measurement frequency reduces the entanglement entropy (green solid curve).

if the time step is a fraction of $\pi$, we expect a special behavior of the monitored evolution, which might be reminiscent of the periodic behavior of the unitary evolution. However, how does the monitored evolution depend on $l$? We will analyze this for $N = 4$ bosons, by comparing $l = 3$ and $l = 4$. Figure 6 visualizes how the ES changes from $J\tau = \pi\hbar/l$ at the center to $(\pi/l \pm 5\times10^{-5})\hbar$ at the boundaries. Figures 6(a) and 6(c) represent the ES for $m = 50$ measurements and Figs. 6(b) and 6(d) the ES for $m = 51$ measurements. There are level degeneracies only at $\pi\hbar/l$, while in the narrow vicinity the levels are well separated and the spectrum is symmetric with respect to $\pi\hbar/l$. It should be noted though that for $l = 4$ [Fig. 6(a)] the lowest level is twofold degenerate, whereas for $l = 3$ [Fig. 6(b)] there is no such a degeneracy. Another remarkable difference between $l = 3$ and $l = 4$ consists in the level change when the number of measurements changes from $m = 50$ [Figs. 6(a) and 6(c)] to $m = 51$ [Figs. 6(b) and 6(d)]. While the two lowest levels for $l = 4$ are not affected by this change, there is a drastic change for $l = 3$. The latter has two low levels for $m = 50$ but three low levels for $m = 51$. The qualitative difference between these two $m$ values reflects the fact that for an odd $l$ only an odd $m$ can satisfy the condition $mJ\tau = 2\pi\hbar$ for periodicity of the phase factor. To understand the effect of this $m$ dependence on the EE, we use the definitions of the ES and the EE in Eqs. (6) and (7) and express the EE by the levels of the ES as

$$\mathcal{S}_2 = -\log_2\left(\sum_{n=0}^{N} e^{-2\xi_{m;n}}\right), \tag{32}$$

where the sum is reminiscent of the sum of Boltzmann weights in statistical mechanics. Therefore, only small values of $\xi_{m;n}$ (i.e., low levels of the ES) contribute substantially to the EE. This means that the EE changes for $m \to m + 1$ when $l = 3$ but it remains unchanged for $l = 4$. This is what we see in Fig. 7. After some fluctuations for small values of $m$, the EE becomes stationary: For $l = 4$ there is just one stationary value [Fig. 7(a)], while for $l = 3$ the EE switches between two stationary values [Fig. 7(b)].

The above analysis relies on the fractional form $J\tau/\hbar = \pi/l$. The behavior of the EE for other values of the time step between measurements can change drastically and may lead to a strongly fluctuating behavior of the EE. In general, repeated measurements have two major effects on the evolution: They

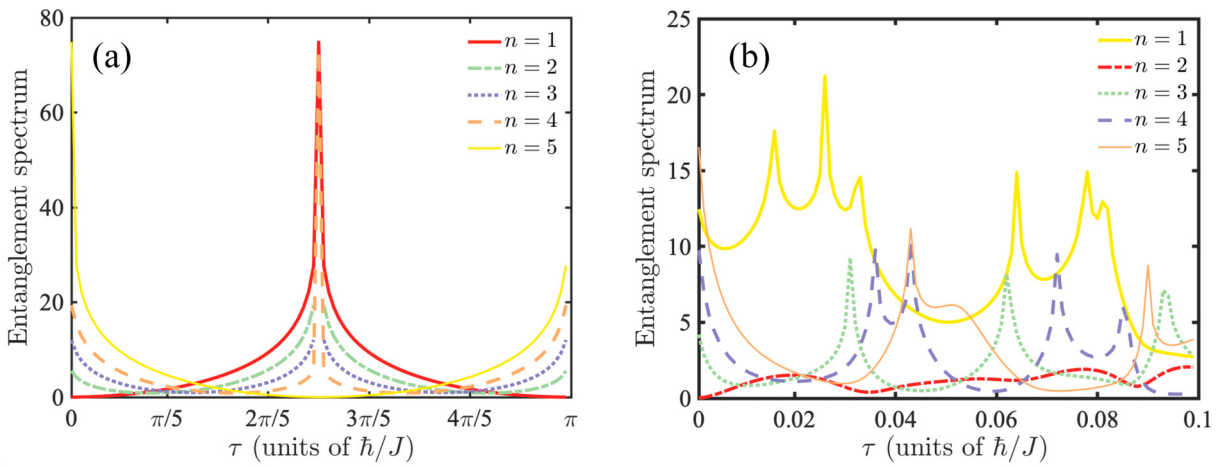


FIG. 5. Entanglement spectrum for the five levels of $N = 4$ bosons for (a) $m = 1$ and (b) $m = 50$ measurements as a function of the time step units $\pi J\tau/\hbar$ and $10^{-3}J\tau/\hbar$, respectively.

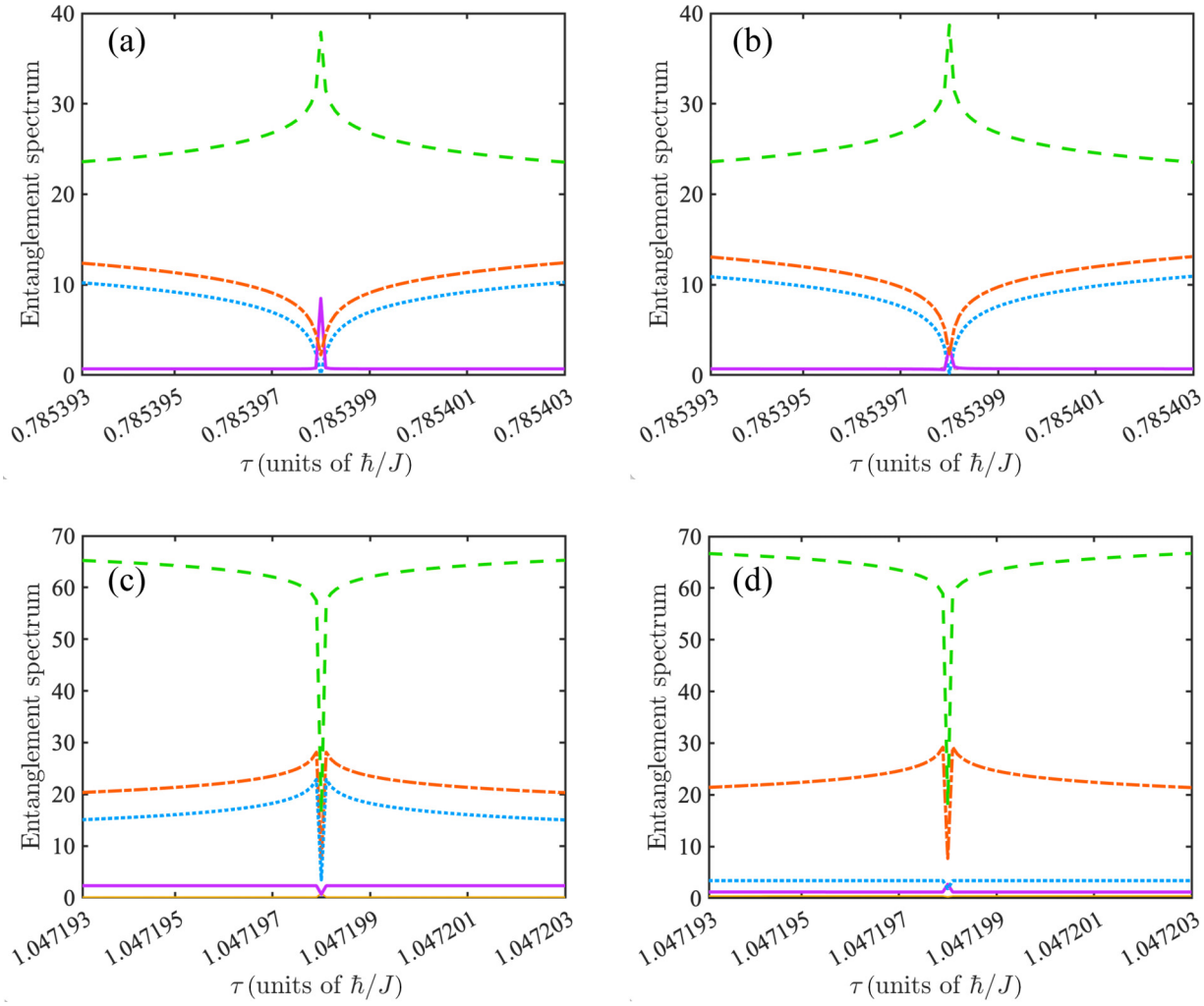


FIG. 6. Entanglement spectrum for $N = 4$ centered around (a) $J\tau = \pi\hbar/4$ and (b) $J\tau = \pi\hbar/3$ for (a) and (c) $m = 50$ and (b) and (d) $m = 51$ measurements. The jump of the green dashed level in (b) causes the switching effect of the entanglement entropy between two values, as illustrated in Fig. 7(b).

destroy the periodicity (recurrence) and they lead to more level crossings in the ES, as illustrated in Fig. 5. The origin of these effects is that the noninteracting bosons are coupled repeatedly in time to the measurement apparatus, which provides an effect similar to a local boson-boson interaction, since the measurement is performed on the same quantum state at different times. The situation can be compared with the unitary evolution of bosons with an interaction $U \neq 0$ in

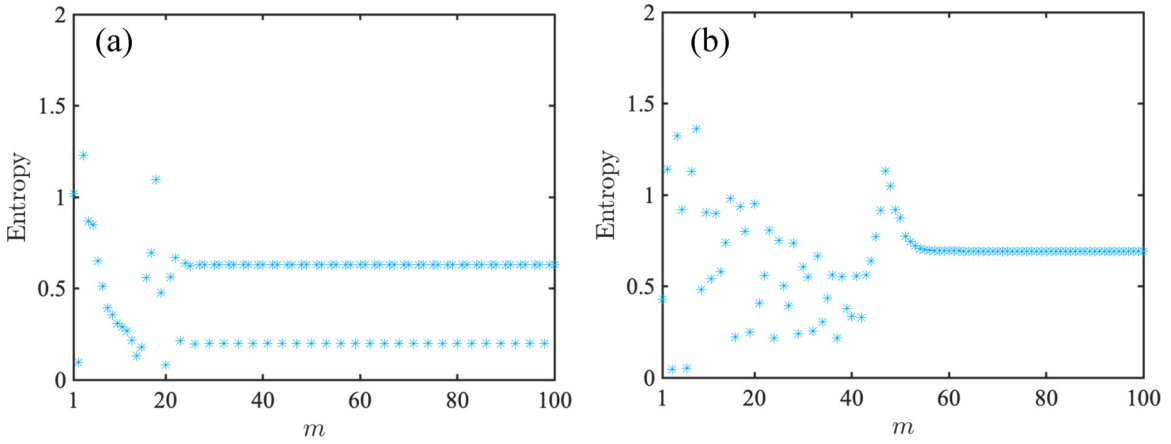


FIG. 7. Plot of the entanglement entropy for $N = 4$ and (a) $J\tau = \pi\hbar/4$ and (b) $J\tau = \pi\hbar/3$.

the Bose-Hubbard Hamiltonian

$$H = -J(a_l^\dagger a_r + a_r^\dagger a_l) + \frac{U}{2}\left(n_l^2 + n_r^2\right). \tag{33}$$

We previously studied this system and found similar behavior of a fluctuating EE and level crossings in the ES [27]. The fluctuations were removed by averaging over time intervals, an approach we could also apply in the present case with $U = 0$. For the monitored evolution we could also introduce random time steps between measurements and average over their distribution [41,46–49]. As a disadvantage of such a time averaging, though, we would not be able to detect the switching of the EE in Fig. 7(b).

## V. CONCLUSION

We have studied the monitored evolution of $N$ noninteracting bosons which tunnel between two wells. The monitoring is carried out by repeated projective measurements. The effect of these measurements is studied in terms of FDR and FDT probabilities to determine quantitatively the monitoring. From the FDR and FDT probabilities we derived the reduced density matrix for one well, the EE, and the ES. This was based on the relation (4) and enabled us to evaluate the EE and the ES directly from the FDR and FDT probabilities. It turns out that the EE is quite sensitive to a change of model parameters, i.e., the number of bosons and the time step between two measurements. The rather complex behavior of the EE indicates that a single quantity, such as the EE, is quite limited for the characterization of the entanglement in the present system. More details were revealed by the ES of Eq. (7). It enabled us to identify the statistical weight of each transition $|0, N\rangle \to |n, N-n\rangle$ to the monitored evolution individually. A characteristic feature of the ES is level crossing. Although it already appears in the unitary evolution [cf. Fig. 5(a)], it becomes much more complex for the monitored evolution in Fig. 5(b). Except for the crossing points, there is always a unique lowest level, representing the dominant transition $|0, N\rangle \to |n, N-n\rangle$. The excitation to higher levels is important as long they are close to the lowest levels. This effect is important when the level $\xi_{m;n}$ changes quickly with $m$. This can happen near the special values $J\tau = \pi\hbar/l$ ($l$ integer), as demonstrated in Fig. 6.

Although our approach was employed only to noninteracting bosons, it is directly applicable to interacting bosons as well. For instance, we can consider the two-site Bose-Hubbard model with the Hamiltonian of Eq. (33). New regimes might appear due to the competition of particle tunneling, particle-particle interaction, and the interaction with the measurement apparatus. This is an ambitious project for the future, in which, among other aspects, the role of Hilbert-space localization should be addressed.


## ACKNOWLEDGMENT

We are grateful to Eli Barkai for useful discussions. This research was supported by the Israel Science Foundation through Grant No. 1614/21 (Q.L.).


## APPENDIX A: EIGENSTATES

With the rotated basis $\{a_\pm, a_\pm^\dagger\}$,

$$a_\pm^\dagger := \tfrac{1}{2}(a_l^\dagger \pm a_r^\dagger), \quad a_\pm = \tfrac{1}{2}(a_l \pm a_r),$$

we obtain, for the tunneling operator $a_l^\dagger a_r + a_r^\dagger a_l$,

$$\begin{aligned} a_l^\dagger a_r + a_r^\dagger a_l &= \tfrac{1}{2}[(a_l^\dagger + a_r^\dagger)(a_l + a_r) - (a_l^\dagger - a_r^\dagger)(a_l - a_r)] \\ &= \tfrac{1}{2}(a_+^\dagger a_+ - a_-^\dagger a_-), \end{aligned} \tag{A1}$$

where $(a_l^\dagger \pm a_r^\dagger)(a_l \pm a_r)$ are number operators. Then we can directly show that $a_+$ and $a_-$ and their Hermitian conjugate commute when $a_l$ and $a_r$ commute. As a consequence, the eigenstate reads

$$|E_k\rangle = \frac{2^{-N/2}}{\sqrt{k!(N-k)!}}(a_+^\dagger)^k (a_-^\dagger)^{N-k}|0, 0\rangle$$

and the application of the tunneling operator yields

$$\tfrac{1}{2}(a_+^\dagger a_+ - a_-^\dagger a_-)|E_k\rangle = (N - 2k)|E_k\rangle.$$

The knowledge of the eigenstates enables us to calculate the spectral weights as scalar products

$$\begin{aligned} q_{n,k} := \langle n, N-n|E_k\rangle &= \frac{2^{-N/2}}{\sqrt{k!(N-k)!}}\langle n, N-n|(a_l^\dagger + a_r^\dagger)^k (a_l^\dagger - a_r^\dagger)^{N-k}|0, 0\rangle \\ &= \frac{2^{-N/2}}{\sqrt{k!(N-k)!}}\langle n, N-n| \sum_{l=0}^{k}\binom{k}{l}(a_l^\dagger)^l (a_r^\dagger)^{k-l} \sum_{l'=0}^{N-k}\binom{N-k}{l'}(a_l^\dagger)^{l'}(-a_r^\dagger)^{N-k-l'}|0, 0\rangle, \end{aligned}$$

and since the left and right operators commute, we obtain, after reordering,

$$\frac{2^{-N/2}}{\sqrt{k!(N-k)!}} \sum_{l=0}^{k}\binom{k}{l}\sum_{l'=0}^{N-k}\binom{N-k}{l'}(-1)^{N-k-l'}\langle n, N-n|(a_l^\dagger)^{l+l'}(a_r^\dagger)^{N-l-l'}|0, 0\rangle. \tag{A2}$$

Due to the orthogonality of the states, the sum vanishes unless $l + l' = n$. Then from the $l$ summation there are two constraints for $l'$, $0 \leqslant l' = n - l$ and $n - l = l' \leqslant N - k$, which are equivalent to $n + k - N \leqslant l \leqslant n$ such that

$$\begin{aligned} n + k - N \leqslant l \leqslant n \quad &\text{for } n + k - N > 0, \\ 0 \leqslant l \leqslant n \quad &\text{for } n + k - N \leqslant 0. \end{aligned}$$

This result, together with $(a^\dagger)^l|0\rangle = \sqrt{l!}|l\rangle$, implies for the scalar product

$$q_{n,k} = 2^{-N/2}\sqrt{\binom{N}{k}\Big/\binom{N}{n}} \times \begin{cases} \sum_{l=0}^{\min\{k,n\}} \binom{k}{l}\binom{N-k}{n-l}(-1)^{N-k-n+l} & \text{for } n+k \leqslant N \\ \sum_{l=n+k-N}^{\min\{k,n\}} \binom{k}{l}\binom{N-k}{n-l}(-1)^{N-k-n+l} & \text{for } n+k > N. \end{cases} \tag{A3}$$

The orthonormal condition of the states $|n, N-n\rangle$ and the states $|E_k\rangle$ lead to

$$\sum_{n=0}^{N} q_{n,k}q_{n,k'} = \delta_{kk'}, \quad \sum_{k=0}^{N} q_{n,k}q_{n',k} = \delta_{nn'}, \tag{A4}$$

respectively.

## APPENDIX B: EXPANSION OF THE FIRST RETURN OR TRANSITION AMPLITUDE

For the FDR or FDT amplitude

$$\phi_{m+1,1} := \langle\psi|(e^{-i\tau H}\Pi)^m e^{-i\tau H}|\psi_0\rangle = \langle\psi|e^{-i\tau H}(\Pi e^{-i\tau H})^m|\psi_0\rangle, \quad \Pi = \mathbf{1} - |\psi_0\rangle\langle\psi_0|, \tag{B1}$$

we obtain two equivalent recursion relations, namely,

$$\phi_{m+1,1} = \phi'_{m,2} - u_1\phi_{m,1} \quad \text{with } \phi'_{m,k} = \langle\psi|e^{-ik\tau H}(\Pi e^{-i\tau H})^{m-1}|\psi_0\rangle,\ u_k = \langle\psi_0|e^{-iHk\tau}|\psi_0\rangle \tag{B2}$$

from the third expression in Eq. (B1) and

$$\phi_{m+1,1} = \phi_{m,2} - \phi_{m,1}v_1 \quad \text{with } \phi_{m,k} = \langle\psi|(e^{-i\tau H}\Pi)^{m-1}e^{-ik\tau H}|\psi_0\rangle,\ v_k = \langle\psi|e^{-iHk\tau}|\psi_0\rangle \tag{B3}$$

from the second expression in Eq. (B1). Then the iteration of Eq. (B2) yields, with $\phi_m \equiv \phi_{m,1}$,

$$\phi_m = v_m - \sum_{j=1}^{m-1} u_{m-j}\phi_j, \quad \phi_1 = v_1, \tag{B4}$$

and from the iteration of Eq. (B3),

$$\phi_m = v_m - \sum_{j=1}^{m-1} \phi_{m-j}v_j, \quad \phi_1 = v_1. \tag{B5}$$

Using the vector notation $\vec{\phi} := (\phi_1, \phi_2, \ldots, \phi_m)$ and $\vec{v} = (v_1, v_2, \ldots, v_m)$, with the matrix $\Gamma$ of Eq. (18) and with the matrix $\hat{\phi} = (\phi_{m-j})$, we can write, for Eqs. (B4) and (B5),

$$(\mathbf{1} + \Gamma)\vec{\phi} = \vec{v}, \quad \vec{\phi} = (\mathbf{1} - \hat{\phi})\vec{v}, \tag{B6}$$

which yields $(\mathbf{1} - \hat{\phi})(\mathbf{1} + \Gamma) = \mathbf{1}$ and Eq. (17), respectively.


[1] F. A. Grünbaum, L. Velázquez, A. H. Werner, and R. F. Werner, Recurrence for discrete time unitary evolutions, Commun. Math. Phys. **320**, 543 (2013).

[2] S. Dhar, S. Dasgupta, and A. Dhar, Quantum time of arrival distribution in a simple lattice model, J. Phys. A: Math. Theor. **48**, 115304 (2015).

[3] S. Dhar, S. Dasgupta, A. Dhar, and D. Sen, Detection of a quantum particle on a lattice under repeated projective measurements, Phys. Rev. A **91**, 062115 (2015).

[4] H. Friedman, D. A. Kessler, and E. Barkai, Quantum renewal equation for the first detection time of a quantum walk, J. Phys. A: Math. Theor. **50**, 04LT01 (2016).

[5] S. Lahiri and A. Dhar, Return to the origin problem for a particle on a one-dimensional lattice with quasi-Zeno dynamics, Phys. Rev. A **99**, 012101 (2019).

[6] R. Yin, K. Ziegler, F. Thiel, and E. Barkai, Large fluctuations of the first detected quantum return time, Phys. Rev. Res. **1**, 033086 (2019).

[7] Q. Liu, R. Yin, K. Ziegler, and E. Barkai, Quantum walks: The mean first detected transition time, Phys. Rev. Res. **2**, 033113 (2020).

[8] Q. Liu, D. A. Kessler, and E. Barkai, Designing exceptional-point-based graphs yielding topologically guaranteed quantum search, Phys. Rev. Res. **5**, 023141 (2023).

[9] L. Bombelli, R. K. Koul, J. Lee, and R. D. Sorkin, Quantum source of entropy for black holes, Phys. Rev. D **34**, 373 (1986).

[10] M. Srednicki, Entropy and area, Phys. Rev. Lett. **71**, 666 (1993).

[11] K. Audenaert, J. Eisert, M. B. Plenio, and R. F. Werner, Entanglement properties of the harmonic chain, Phys. Rev. A **66**, 042327 (2002).

[12] J. Eisert, M. Cramer, and M. B. Plenio, *Colloquium*: Area laws for the entanglement entropy, Rev. Mod. Phys. **82**, 277 (2010).

[13] Q. Miao and T. Barthel, Eigenstate entanglement: Crossover from the ground state to volume laws, Phys. Rev. Lett. **127**, 040603 (2021).

[14] L. Amico, R. Fazio, A. Osterloh, and V. Vedral, Entanglement in many-body systems, Rev. Mod. Phys. **80**, 517 (2008).

[15] D. A. Abanin, E. Altman, I. Bloch, and M. Serbyn, *Colloquium*: Many-body localization, thermalization, and entanglement, Rev. Mod. Phys. **91**, 021001 (2019).

[16] G. Vidal, J. I. Latorre, E. Rico, and A. Kitaev, Entanglement in quantum critical phenomena, Phys. Rev. Lett. **90**, 227902 (2003).
[17] P. Calabrese and J. Cardy, Entanglement entropy and quantum field theory, J. Stat. Mech. (2004) P06002.
[18] I. Peschel and V. Eisler, Reduced density matrices and entanglement entropy in free lattice models, J. Phys. A: Math. Theor. **42**, 504003 (2009).
[19] P. Calabrese and J. Cardy, Entanglement entropy and conformal field theory, J. Phys. A: Math. Theor. **42**, 504005 (2009).
[20] M. Serbyn, Z. Papić, and D. A. Abanin, Criterion for many-body localization-delocalization phase transition, Phys. Rev. X **5**, 041047 (2015).
[21] R. Nandkishore and D. A. Huse, Many-body localization and thermalization in quantum statistical mechanics, Annu. Rev. Condens. Matter Phys. **6**, 15 (2015).
[22] P. Kos, M. Ljubotina, and T. Prosen, Many-body quantum chaos: Analytic connection to random matrix theory, Phys. Rev. X **8**, 021062 (2018).
[23] A. Chan, A. De Luca, and J. T. Chalker, Solution of a minimal model for many-body quantum chaos, Phys. Rev. X **8**, 041019 (2018).
[24] Y. Li, X. Chen, and M. P. A. Fisher, Measurement-driven entanglement transition in hybrid quantum circuits, Phys. Rev. B **100**, 134306 (2019).
[25] B. Skinner, J. Ruhman, and A. Nahum, Measurement-induced phase transitions in the dynamics of entanglement, Phys. Rev. X **9**, 031009 (2019).
[26] O. Lunt, M. Szyniszewski, and A. Pal, Measurement-induced criticality and entanglement clusters: A study of one-dimensional and two-dimensional Clifford circuits, Phys. Rev. B **104**, 155111 (2021).
[27] Q. Liu and K. Ziegler, Entanglement transition through Hilbert-space localization, Phys. Rev. A **107**, 012413 (2023).
[28] A. Bulgac, Entanglement entropy, single-particle occupation probabilities, and short-range correlations, Phys. Rev. C **107**, L061602 (2023).
[29] A. Bulgac, M. Kafker, and I. Abdurrahman, Measures of complexity and entanglement in many-fermion systems, Phys. Rev. C **107**, 044318 (2023).
[30] S. Tornow and K. Ziegler, Measurement-induced quantum walks on an IBM quantum computer, Phys. Rev. Res. **5**, 033089 (2023).
[31] Y. Minoguchi, P. Rabl, and M. Buchhold, Continuous Gaussian measurements of the free boson CFT: A model for exactly solvable and detectable measurement-induced dynamics, SciPost Phys. **12**, 009 (2022).
[32] T. E. Lee and M. C. Cross, Quantum-classical transition of correlations of two coupled cavities, Phys. Rev. A **88**, 013834 (2013).
[33] S. Haroche, M. Brune, and J. M. Raimond, From cavity to circuit quantum electrodynamics, Nat. Phys. **16**, 243 (2020).
[34] W. Löffler, T. G. Euser, E. R. Eliel, M. Scharrer, P. St. J. Russell, and J. P. Woerdman, Fiber transport of spatially entangled photons, Phys. Rev. Lett. **106**, 240505 (2011).
[35] Y. Kang, J. Ko, S. M. Lee, S.-K. Choi, B. Y. Kim, and H. S. Park, Measurement of the entanglement between photonic spatial modes in optical fibers, Phys. Rev. Lett. **109**, 020502 (2012).
[36] H. Cao, S.-C. Gao, C. Zhang, J. Wang, D.-Y. He, B.-H. Liu, Z.-W. Zhou, Y.-J. Chen, Z.-H. Li, S.-Y. Yu, J. Romero, Y.-F. Huang, C.-F. Li, and G.-C. Guo, Distribution of high-dimensional orbital angular momentum entanglement over a 1 km few-mode fiber, Optica **7**, 232 (2020).
[37] Y. Aharonov, L. Davidovich, and N. Zagury, Quantum random walks, Phys. Rev. A **48**, 1687 (1993).
[38] J. Bourgain, F. A. Grünbaum, L. Velázquez, and J. Wilkening, Quantum recurrence of a subspace and operator-valued Schur functions, Commun. Math. Phys. **329**, 1031 (2014).
[39] H. Friedman, D. A. Kessler, and E. Barkai, Quantum walks: The first detected passage time problem, Phys. Rev. E **95**, 032141 (2017).
[40] H. Li and F. D. M. Haldane, Entanglement spectrum as a generalization of entanglement entropy: Identification of topological order in non-Abelian fractional quantum Hall effect states, Phys. Rev. Lett. **101**, 010504 (2008).
[41] K. Ziegler, E. Barkai, and D. Kessler, Randomly repeated measurements on quantum systems: Correlations and topological invariants of the quantum evolution, J. Phys. A: Math. Theor. **54**, 395302 (2021).
[42] G. J. Milburn, J. Corney, E. M. Wright, and D. F. Walls, Quantum dynamics of an atomic Bose-Einstein condensate in a double-well potential, Phys. Rev. A **55**, 4318 (1997).
[43] B. Yurke and D. Stoler, Generating quantum mechanical superpositions of macroscopically distinguishable states via amplitude dispersion, Phys. Rev. Lett. **57**, 13 (1986).
[44] S. Haroche and J.-M. Raimond, *Exploring the Quantum: Atoms, Cavities, and Photons* (Oxford University Press, Oxford, 2006).
[45] B. Misra and E. C. G. Sudarshan, The Zeno's paradox in quantum theory, J. Math. Phys. **18**, 756 (1977).
[46] D. Das, S. Dattagupta, and S. Gupta, Quantum unitary evolution interspersed with repeated non-unitary interactions at random times: The method of stochastic Liouville equation, and two examples of interactions in the context of a tight-binding chain, J. Stat. Mech. (2022) 053101.
[47] D. Das and S. Gupta, Quantum random walk and tight-binding model subject to projective measurements at random times, J. Stat. Mech. (2022) 033212.
[48] A. Acharya and S. Gupta, Tight-binding model subject to conditional resets at random times, Phys. Rev. E **108**, 064125 (2023).
[49] M. Kulkarni and S. N. Majumdar, First detection probability in quantum resetting via random projective measurements, J. Phys. A: Math. Theor. **56**, 385003 (2023).